ISSN 0029 - 3865

CBPF-NF-030/85

THE EFFECT OF THE H_2O/TEOS RATIO ON THE STRUCTURE OF GELS DERIVED BY THE ACID CATALYSED HYDROLYSIS OF TETRAETHOXYSILANE

by

I. Strawbridge*, A.F. Craievich and P.F. James*

Centro Brasileiro de Pesquisas Físicas - CBPF/CNPq
Rua Dr. Xavier Sigaud, 150
22290 - Rio de Janeiro RJ, Brasil

*Department of Ceramics, Glasses and Polymers
The University of Sheffield
S10 2TZ, UK

Abstract

Silica gels were produced by the acid catalysed hydrolysis of tetraethoxysilane (TEOS) using H_2O/TEOS ratios from 2 to 50. After heat treatment the structure of the gels was studied using nitrogen adsorption, small angle X-ray scattering (SAXS), transmission electron microscopy (TEM) and bulk density measurements.

All the gels possessed microporosity in the region of 30 Å or less. For H_2O/TEOS = 25 and 50 the matrix density was found to be uniform, but for gels from solutions with H_2O/TEOS = 2, 4 and 10, density fluctuations in the matrix were detected from a Porod analysis of the SAXS data. These results indicate that in high water content solutions, rearrangement of the polymeric chains leads to small densified particles, but for lower water content solutions, gelation results from the entanglement of linear chains leaving free volume on a molecular scale between the chains.

Key words: Sol-gel glasses; SAXS; Microporosity.

Introduction

The initial water content used for the acid catalysed hydrolysis of ethanolic solutions of tetraethoxysilane (TEOS) has been found to have an effect on their ability to produce monolithic gels. Generally, larger monolithic gels are produced from solutions with high initial H_2O/TEOS mole ratios [1] whereas solutions more suitable for the production of fibres and coatings are derived from low H_2O/TEOS ratios [2]. The aim of the present project was to establish the reasons for these differences by investigating the structure of gels prepared from solutions with various initial H_2O/TEOS ratios. The four main techniques employed to characterize the gels were nitrogen adsorption , small angle X-ray scattering, transmission electron microscopy and bulk density measurements.

Gas adsorption has been used frequently in the past to determine the surface areas, pore size distributions and their variation with temperature for bulk materials prepared by the sol-gel process [3-10]. However some care should be taken in the case of isotherms of type I (from the classification of Brunauer et al. [11]) which are indicative of adsorption by a microporous solid, i.e., a solid with pores around 20 Å in diameter. Reference to Gregg and Sing [12] demonstrates that surface areas calculated using the BET [13] and Langmuir [14] techniques are of dubious validity and the accuracy of pore size distributions can also be questioned. Pore volumes can be reliably determined, however, either from the adsorbate uptake at the plateau of the type I isotherm or from standard isotherm techniques [15,16].

The majority of previous small angle X-ray scattering studies have concentrated on the study of heterogeneities in solution [9,17,18], although mean pore diameters have been quoted by Yu et al. [19] for silica

gels derived from tetraethoxysilane. Yoldas [8] has also quoted SAXS results for alumina gels. Interpretation of the scattering curves has generally involved Guinier's law [20], but Porod's law [21] has also been employed.

Several studies have included the monitoring of bulk and true densities as a function of temperature using various pyknometric methods [3,4,7,19,22].

Another important technique for the characterization of gels is electron microscopy. Specimen preparation methods for transmission microscopy have included dropping the hydrolysed solutions onto carbon coated grids [3], platinum-palladium pre-shadowed carbon replicas [3], gel fragmentation [17], and ion-beam thinning [23]. For alkoxide derived silica gels, a fundamental difference in the microstructure of gels from acid and base catalysis has been demonstrated. Acid catalysis yielded gels with extremely fine microstructural features which showed no particulate nature, whereas base catalysis produced gels with a coarse particulate microstructure [3,17].

Experimental

Gel preparation

Ethanolic solutions of tetraethoxysilane (TEOS) were prepared with a range of H_2O/TEOS ratios. The components are presented in Table 1 in the order of mixing. After stirring for 1 hour the solutions were poured into glass dishes, covered by plastic film and left to gel at room temperature. Table 2 gives the calculated molarities of these solutions.

The gels were allowed to contract at room temperature until they were free of the walls of the containers. Drying was then performed at 50°C, prior to heating at 1°C/min to the required temperature and holding for 1 hour with a flow of oxygen through the furnace.

Characterization Techniques

Nitrogen adsorption

The adsorption isotherms for the coarsely ground gels were determined at 77 K using a volumetric technique with nitrogen as the adsorbate. The samples were outgassed for 8 hours at 120°C. Therefore, the lowest heat treatment temperature examined was 150°C. The isotherms presented here have been corrected for the non-ideality of nitrogen at low temperatures.

Small Angle X-ray Scattering

The SAXS measurements were performed on thin specimen foils at the scattering station of the synchroton radiation laboratory, LURE, Orsay, Université Paris-Sud. Pin-hole collimation was employed using radiation with a wavelength of 1.608 Å. After correcting for parasitic scattering the curves were normalized to equivalent sample thicknesses and X-ray beam intensities.

Bulk Density Measurements

The bulk densities of the gels were determined using a mercury displacement technique. A sample chamber of known volume containing a known weight of sample was evacuated to better than 0.1 torr before it was filled to a repeatable level in a uniform capillary using mercury from a weighing bottle. Atmospheric pressure was restored to the mercury surface forcing the displacement liquid into pores greater than 14 μm diameter. The volume of the sample was then calculated from the change in weight of

the mercury bottle, the fall in mercury level on admitting air and the volume of the empty sample chamber. With a specimen volume of 0.2 cm^3 density could be determined to within ± 0.02 $g.cm^{-3}$.

Transmission Electron Microscopy

The gels were examined in the electron microscope in the form of ion beam thinned foils. The materials were first reduced to 15 μm foils by conventional grinding and polishing techniques. A hole in the foil was then produced by bombardment with 5 kV Argon ions in an Edwards IBM A2 ion beam thinning apparatus.

Results

Nitrogen Adsorption Studies

The nitrogen adsorption isotherms at 77 K for the series of heat treated gels prepared from a solution containing $H_2O/TEOS = 2$ (designated $SiO_2.2H_2O$) are shown in Figure 1. The isotherms are of type I of the BET classification [13], which is indicative of a microporous solid with pore widths below 20 Å. The plateau in the adsorption can be seen to fall with increasing heat treatment temperature, only slightly between 150 and 400°C, but more rapidly at higher temperatures. At high relative pressures ($p/p_0 > 0.97$), upturns in the isotherms are apparent, which are usually assigned to capillary condensation in macropores ($d \gtrsim 200$ Å).

Figure 2 shows the isotherms for gels prepared from solutions with different water contents after heating to 650°C. Again type I isotherms were produced and a dependence on water content is apparent for the plateau height and the sharpness of the knee. The reduction in this sharpness with increasing $H_2O/TEOS$ ratio suggests a shift to larger pores [12].

Although surface areas have been quoted in the past for gels giving type I isotherms using the Langmuir and BET treatments their validity is subject to some doubt [12]. Therefore analysis has been restricted to standard isotherm techniques, which enable the separation of the contribution to the adsorption isotherm of multilayer coverage and capillary condensation from that of micropore filling. By choice of a suitable standard isotherm from a non-porous solid with a chemically similar surface, reliable estimates can be made from a type I isotherm for the micropore volume as well as the remaining external surface, if the amount of gas adsorbed by the sample at a given relative pressure is plotted against the number of moles of gas, N, adsorbed by the standard at the same pressure. In the method of Sing (16), the amount of gas adsorbed by the standard is expressed in terms of N/N_s ($= \alpha_s$), where N_s is the number of moles adsorbed at $p/p_0 = 0.4$. The reference solid chosen was Fransil EL, a non-porous hydroxylated silica, whose adsorption isotherm for nitrogen at 77 K was reported by Carruthers et al [24]. Selected α_s plots for the $SiO_2.2H_2O$ series of gels are presented in Figure 3.

The steep region of the curves for $\alpha_s \gtrsim 1$ are the result of micropore filling and the almost horizontal lines are due to multilayer covering of surface not in micropores. Extrapolation of the multilayer region to $\alpha_s = 0$ defines the amount of nitrogen to fill micropores and assuming the nitrogen is in a form similar to bulk liquid the micropore volume can be calculated. The surface area not in micropores is proportional to the small (but non-zero) gradient of the multilayer region.

Table 3 gives the values for micropore volume and surface area not included in micropores for the $SiO_2.2H_2O$ samples and for the gels with different H_2O/TEOS ratios after heating to 650°C. The surface area not in

micropores is very small with no systematic variation. This is not surprising since there was no attempt to control exactly the particle size used in these experiments, but it was generally quite large (50-500 μm).

The presence of some macroporosity ($d \gtrsim 200$ Å) is suggested by the slight upturn in the isotherm at high relative pressures ($p/p_0 \gtrsim 0.97$) and an estimate of the volume can be made by assuming pore filling is occurring during the upturn region and the adsorbate is in a form similar to bulk liquid. The final column of Table 3 contains these values which are small compared with the micropore volumes.

Small Angle X-ray Scattering

Difficulties were encountered in preparing a complete set of specimens which remained defect free during heat treatment and during the polishing stages, therefore an incomplete set of scattering curves was obtained. Sufficient results were produced, however, to allow correlation with the results from gas adsorption and bulk density measurements. Figure 4 shows a representative series of scattering curves for gels after heating to 650°C, which were derived from solutions with different initial H_2O/TEOs ratios. Except for the gel with H_2O/TEOS = 25 all these curves show a maximum in the SAXS intensity. A maximum was also obtained for all the other curves not shown in Figure 4.

The maximum in the scattering curves indicates the presence of a densely packed system of heterogeneities and under such conditions the Guinier approximation is of reduced validity and should only be used to determine orders of magnitude of particle or pore sizes from the scattering data [25].

An alternative measure of the average size of heterogeneities (particles or voids) can be obtained from the correlation length ℓ_c [26], which is defined as the average value of the lengths of chords drawn in all directions and through all points in the heterogeneities. This parameter can be calculated from the scattering data using the expression:

$$\ell_c = \pi \int_0^\infty I(h)hdh / \int_0^\infty I(h)h^2dh \qquad [1]$$

where h is the modulus of the scattering vector ($h = (4\pi Sin\theta)/\lambda$, 2θ being the scattering angle and λ the radiation wavelength).

Compared with the radius of gyration obtained from the Guinier approximation, the correlation length is not as sensitive to changes in the packing density of heterogeneities and therefore the values of ℓ_c are likely to be closer to the their average size.

The scattering data was also analysed at large angles using Porod's law which is valid for any shape of heterogeneity, so long as the orientations are random and none of the dimensions approach zero (e.g. needles or plates). It is also valid for dissimilar heterogeneities and for a close-packed system. Systematic deviations from Porod's law can occur when there are density fluctuations in the phases or when the interface is not well defined. In the first case, the deviation is positive, in the second, negative. Plotting $h^4I(h)$ versus h we have a positive deviation when the slope is positive at large h and a negative deviation for a negative slope. In the case of voids, it is evident that a fluctuation in density can only exist in the matrix. Assuming that there is a step discontinuity of the electron density at the void interface, we have for three-dimensional fluctuations [27]:

$$\lim_{h \to \infty} \frac{h^4 . I(h)}{Q_0} = S_v \cdot \frac{1}{\pi \phi_1 \phi_2} + Fh^4 \qquad [2]$$

where $Q_0 = \int_0^\infty h^2 I(h)dh$, S_v is the surface area of the matrix-void interface per unit volume, ϕ_1 and ϕ_2 are the volume fractions of the voids (pores) and matrix respectively, and F is the fluctuation parameter which measures the magnitude of the density fluctuations in the matrix [27]. If an experimental plot of $h^4I(h)/Q_0$ versus h^4 shows an asymptotic linear behaviour $a + bh^4$, we can determine from it a "surface parameter" $S_v' = a\pi$. The specific surface area of the interface per unit mass, S, can be obtained by the following equation [26]:

$$S = S_v' \phi_1(1 - \phi_1)/\rho \qquad [3]$$

where ρ is the bulk density of the sample. In order to determine S, the volume fraction of the voids ϕ_1 and the bulk density ρ must be obtained by independent techniques. The slope b of the straight line yields the fluctuation parameter F.

If a plot of $h^4I(h)/Q_0$ versus h^4 gives a positive slope at large h, this is strong evidence that the matrix phase possesses density fluctuations, i.e. it has defects or very small voids with sizes on the molecular scale. If the slope is zero at large h i.e. F = 0, this implies that the matrix density is homogeneous and Porod's law is obeyed. Figure 5 shows $h^4I(h)$ plotted against h^4 for the gels after heating to 650°C. Here Porod's law is approximately obeyed or deviated from slightly by the high water containing gels (H_2O/TEOS = 25 and 50), but strong deviations occur for the low water content gels (H_2O/TEOS = 2, 4 and 10).

Figure 6 shows the correlation length ℓ_c and the surface parameter S_v' as a function of the H_2O/TEOS ratio and Figure 7 illustrates the variation of the matrix fluctuation parameter F with the H_2O/TEOS ratio. Table 4 contains the numerical values derived from the SAXS measurements.

Bulk Density

The bulk densities measured after different heat treatments for silica gels derived from solutions with different initial H_2O/TEOS ratios are given in Table 5.

Transmission Electron Microscopy of Bulk Gels

Specimens of the gels from solutions with an initial H_2O/TEOS ratio of 2 were examined by TEM after heating to various temperatures. For treatments between 85 and 800°C, a layered structure was observed with typical dimensions between the edges of the overlapping layers around 200 nm. However, on a finer scale the materials were essentially featureless. Little change in structure was detected between gels dried at 85°C, (Figure 8) and gels heated at temperatures up to 800°C, but a sample heated to 850°C showed the initial signs of bloating with the production of spherical cells possessing diameters in the region 2-3 μm (Figure 9). After heating to 900°C, this material was found to have severely fractured and bloated.

Samples produced from solutions with higher water contents were also examined after treatment at low temperatures. Again a layered structure was observed and no fine structure could be detected.

Discussion

Proposed model for the effect of initial H_2O/TEOS ratio on the formation of silica gels

Low Water Content: H_2O/TEOS = 2

The studies of Brinker et al. (9) showed that essentially linear chains consisting of fully esterified units with only weak cross-linking resulted when tetraethoxysilane was hydrolysed in acidic solution using a

H_2O/TEOS ratio equal to 1. This was explained by simple steric arguments; monomers are more readily hydrolysed than dimers or chain end groups, which are in turn more readily hydrolysed than middle groups in chains.

The H_2O/TEOS ratio of 2 in the present case is insufficient for complete hydrolysis. Therefore, the reaction product for such low initial water contents is expected to be similar to that found by Brinker and coworkers, i.e. linear chains with residual alkoxy groups. These organic species would be expected to influence the packing of chains during gelation and subsequent treatments.

Intermediate Water Content: H_2O/TEOS = 4 and 10

Sufficient water is provided in the solutions for complete hydrolysis of the alkoxide. Evidence for the hydrolysis going to completion is provided by the studies of Aelion et al [28]. They found that the number of moles of water consumed per mole of alkoxide approached four (for comparable water contents in ethanol as solvent) using acid concentrations greater than 0.003 M. Initial growth would still be expected via linear chain formation, but due to the higher concentration of polymer (cf. the high water concentration case) intermolecular reactions are more likely than intramolecular reactions. Gelation would occur by the entanglement of the linear species to give very small overlapped clusters as suggested by Brinker et al. [9], which aggregate and lead to a gel with a higher density than would be expected if a) there was a low packing density of chains caused by incomplete hydrolysis or b) the packing of larger spherical particles had caused gelation.

High Water Content: H_2O/TEOS = 25 or 50

Again complete hydrolysis would be expected by virtue of the high concentration of water in the solution. However the excess of water would also be expected to influence the subsequent condensation reactions. The

initial growth is assumed to lead to linear chains, but the high dilution in water results in cyclization since the probability of intramolecular reaction is increased with respect to intermolecular reaction. The reaction mechanism under such conditions is similar to the polymerization of silicic acid in aqueous solution at low pH as described by Iler [29]. Rearrangement of the cyclic species gives small densified particles which act as nuclei for further growth via an Oswald ripening mechanism. Under acidic conditions the rates of polymerization and depolymerization are slow, therefore particle growth becomes negligible after a size of 2-4 nm is reached.

Gelation then occurs by the development of a three-dimensional network of such particles. The porosity of such gels is located in the interstices caused by the packing of the approximately spherical particles.

Combination of the Results from Nitrogen Adsorption, Bulk Density and TEM Studies

If all the porosity in these samples is accessible to the adsorbate in the nitrogen adsorption experiments, a total pore volume can be calculated. Therefore, if these results are combined with the values for bulk density, ρ_{bulk}, an estimate of the matrix density, ρ_{matrix}, can be made using the equation:

$$\frac{1}{\rho_{matrix}} = \frac{1}{\rho_{bulk}} - V_{\mu p} - V_{mp} \qquad [4]$$

where $V_{\mu p}$ and V_{mp} are the specific micropore and macropore volumes respectively.

Table 6 shows the results of this calculation. The final column contains the value of the unaccounted volume V_u assuming that the matrix density was that of fully densified silica, i.e. 2.2 g/ml, using the expression:

$$V_u = \frac{1}{\rho_{bulk}} - \frac{1}{2.2} - V_{\mu p} - V_{mp} \qquad [5]$$

The values for the unaccounted volume of the $SiO_2.2H_2O$ gels are clearly significant in relation to the measured micropore volume and large compared with the macropore volume. Only the unaccounted volume of the 300°C sample could be explained by the maximum error in the bulk density measurement (within ±0.02 g/ml). Therefore, the general conclusion is that the matrix is not fully densified for this series of gels. It is not clear from these measurements, however, whether the slightly lower density of the matrix is due to isolated porosity or free volume on a molecular scale. Using the information obtained from electron microscopy, there would appear to be no large scale isolated porosity. Therefore, free volume between the molecular chains seems to be the most likely explanation. In addition, the macropore volume could be located in or around the overlap regions of the layered structure as seen by TEM.

A similar analysis has been applied to the adsorption and bulk density data from samples PS3 and PS4 after heating to 650°C. These results are also presented in Table 6. For these gels the matrix density is close to that of vitreous silica. Therefore, in this case it is reasonable to conclude that a fully densified matrix has been formed and all the voids can be attributed to the micro- and macroporosity determined by gas adsorption.

Again, from TEM no fine structure was detected and only the larger layered structure was observed, which again could be the cause of the macroporosity detected on the isotherms.

The variation of bulk densities with the initial water content of the solution (Table 5) is also consistent with the proposed model. Low density gels are formed a) when incomplete hydrolysis occurs because of low initial water content or b) when cyclization and particle formation result from high dilution in solutions with high initial water contents. In case a), the free volume is located around the chains, whereas in case b) larger interstices caused by the packing of spheres would account for the free volume. The high density gels occur under conditions where complete hydrolysis is expected and gelation is caused by the aggregation of very small clusters as a result of the entanglement and crosslinking of chains (9).

Similar results have been obtained by Krol and van Lierop (7) for a silica gel from a solution with $H_2O/TEOS \simeq 10$ and with similar concentrations of components. After drying at 120°C, Krol and van Lierop found a density of 1.38 g/ml and a type I isotherm was obtained with nitrogen as adsorbate. Extrapolation of the plateau region of their isotherm gives an approximate micropore volume of 0.25 ml/g. Using equation [5] this material would also appear to have porosity which is not accessible to nitrogen ($V_u \simeq 0.02$ ml/g).

The bloating phenomena can also be explained by this model. Only samples with $H_2O/TEOS \geq 25$ remained in large pieces after heating above 750°C and as the initial water content was reduced, bloating became a more severe problem. The absence of bloating for samples with high water content can be attributed to the larger pores which allow the condensation products, chiefly water, to escape prior to pore closure. The smaller

pores in the lower H_2O/TEOS gels close at lower temperatures trapping any residual water, which tries to expand during further heating, thus causing cracking or bloating.

The differences in the densification behaviour for gels from solutions with different initial H_2O/TEOS ratios suggest that the gels with the smallest pores sinter at lower temperatures, but it is difficult to draw more detailed conclusions.

Correlation with Small Angle X-ray Scattering

The increase in the mean size of heterogeneities (as measured by the correlation length ℓ_c, Figure 6) with increasing water content in the starting solution is consistent with the variation in shape of the adsorption isotherms and the model proposed for the gel structure.

The structural model divides the H_2O/TEOS ratio into three ranges:

a) Low water content (e.g. H_2O/TEOS = 2)

The behaviour here is too complex to allow meaningful structural features to be inferred from the SAXS results, since the model assumes a system with more than two densities, i.e. the weakly crosslinked polymer with the after-effects of residual alkoxy groups and microporosity.

b) Intermediate Water Content (e.g. H_2O/TEOS = 4 and 10

In this range the gels may be regarded as "two density systems" consisting of pores dispersed in an imperfect matrix of crosslinked linear polymers and pores.

c) High Water Content (e.g. $H_2O/TEOS = 25$ and 50)

Again a "two density system" is assumed, but it is composed of pores dispersed in an approximately perfect matrix of spherical silica particles.

These structural features may now be used to make sense of the Porod behaviour of the SAXS curves. The fluctuation parameter F (Figure 7) and surface parameter S_v' (Figure 6) both show an overall tendency to decrease with increasing $H_2O/TEOS$ ratio. The changes in F are very marked and indicate that the gels from solutions with high initial water contents are composed of a "two density system" of pores in an approximately perfect matrix, while the lower water content solutions give gels consisting of pores in an imperfect matrix with density fluctuations. These fluctuations may then be associated with free volume between the molecular chains which gave the unaccounted volume when the nitrogen adsorption results were compared with the bulk densities. Furthermore, qualitative agreement is found for the unaccounted volume of 0.0049 ml/g for $H_2O/TEOS = 25$ and zero for $H_2O/TEOS = 50$ with the small and zero values of F for $H_2O/TEOS = 25$ and 50 respectively.

Although large and positive, the F value for $H_2O/TEOS = 2$ does not fit in with the general trend of decreasing F with increasing $H_2O/TEOS$ ratio. However, as explained previously, there is an additional compliction at low water content, the presence of residual alkoxy groups. Although these groups would have been removed with treatment to 650°C they would be expected to influence the resulting structure. In fact the value of F indicates a density fluctuation in the matrix, correlating with the unaccounted volume found from the earlier studies.

The decreasing values of the parameter S_v' with increasing water content can be understood in terms of the increasing correlation length ℓ_c (Figure 6). The specific surface area S can be determined from equation [3] using the measured bulk density (P) and the volume fraction ϕ_1 of voids calculated from the micropore volume determined by gas adsorption. Table 7 contains the specific surface areas for $H_2O/TEOS$ = 2, 25 and 50 after heating to 650°C and for $H_2O/TEOS$ = 2 after heating to 750°C. The surface areas can be seen to reduce slightly for increasing $H_2O/TEOS$ ratio in the starting solution.

The pore fraction ϕ_1 and bulk density ρ values from the high water content gels (Table 7) correspond quite closely to the values obtained by Avery and Ramsay (30) for the primitive hexagonal packing of silica spheres with a coordination number of 8. They found a pore fraction of 0.395 and a density of 1.33 g/ml and given a particle radius, R, the radius of the spheres inscribed in the cavities was shown to be 0.527R. The radius of particles R (in nm) can then be calculated from the specific surface S (in m^2/g Table 7) and the coordination number n using the expression:

$$SR^2 - 1375R + 128.9\ n = 0 \qquad [6]$$

Table 8 shows the values for particle diameter 2R and pore diameter (= 1.054R).

The pore sizes can be seen to be in close agreement with the correlation length ℓ_c calculated from the SAXS data. The dimensions of the particles are approximately at the resolution limit of the electron microscope employed in the present work, therefore their detection would not be expected.

Influence of Temperature

The structural parameters from SAXS (Table 4) derived from samples heated at different temperatures for equivalent initial water contents in general showed little variation. In particular, the SAXS results did not show a decrease in mean void size as was suggested by the change in shape of the adsorption isotherms of the gels from solutions with $H_2O/TEOS = 2$. However, the P values did show some variations with temperature and indicated a trend towards densification of the matrix as the heat treatment temperature was raised (Table 4). This was particularly noticeable in the case of PS1 and PS2 ($H_2O/TEOS = 4$ and 10).

Conclusions

Results obtained from nitrogen adsorption, bulk density, TEM and SAXS studies indicated that the degree of hydrolysis and the dilution of solutions play an important role in determining the structure of gels obtained by the acid catalysed hydrolysis and polymerization of tetraethoxysilane solutions.

The majority of the porosity in these gels was around 30 Å or less in diameter according to the nitrogen adsorption isotherms which, along with the SAXS correlation length ℓ_c, suggested slightly larger voids for gels from solutions with high initial water contents compared with gels from low water content solutions.

Analysis of the SAXS data using Porod's law indicated that gels from solutions with $H_2O/TEOS = 2$, 4 and 10 have an imperfect matrix with density fluctuations while for $H_2O/TEOS = 25$ and 50 the matrix density is approximately uniform. Correlation of the bulk density measurements and nitrogen adsorption studies showed an inaccessible free volume for low $H_2O/TEOS$ ratios but no such free volume for $H_2O/TEOS = 25$ and 50.

These observations for the low H_2O/TEOS gels are consistent with free volume on a molecular scale and consistent with the proposed model where gelation occurred by the aggregation of small clusters produced by the entanglement of linear chains which are poorly hydrolysed for H_2O/TEOS = 2 or fully hydrolysed for H_2O/TEOS = 4 and 10. The microporosity would then be located between the very small clusters. Higher H_2O/TEOS ratios have the effect of producing what is virtually an aqueous system, thus diluting the solution so that intramolecular reactions become more likely and the cyclic species lead to particle formation. These particles are highly densified thus eliminating the molecular size free volume, but voids still exist on the micropore scale between particles. The bulk density and the volume fraction of pores for the high water content gels were correlated with the values calculated for a system of densified silica spheres with a coordination number around 8. The surface area calculated from SAXS was then used to obtain an approximate particle diameter of 50 A and a pore diameter of 26 A. This is close to the void size obtained from the SAXS correlation length ℓ_c.

The macroporosity from the nitrogen adsorption was probably associated with the layered structure seen in the TEM, but this would not be expected to be detected by X-ray scattering.

Acknowledgement

I. Strawbridge wishes to thank the British Technology Group for providing financial support for his Research Studentship at the University of Sheffield.

Figure Captions

Figure 1 — Nitrogen adsorption isotherms measured at 77K for $SiO_2.2H_2O$ gels after heating to various temperatures at 1°C/min and holding for 1 hour.

Figure 2 — Nitrogen adsorption isotherms measured at 77K for silica gels from solutions of different water content after heating to 650°C at 1°C/min and holding for 1 hour.

Figure 3 — α_s Plots for $SiO_2.2H_2O$ gels after heating to various temperatures.

Figure 4 — Small angle X-ray scattering curves for silica gels prepared from solutions with different H_2O/TEOS ratios after heating to 650°C.

Figure 5 — Porod plots for silica gels prepared from solutions with different H_2O/TEOS ratios after heating to 650°C.

Figure 6 — Graphs of SAXS correlation length and surface parameter as a function of H_2O/TEOS ratio for silica gels after heating to 650°C.

Figure 7 — Variation of the matrix density fluctuation parameter with the H_2O/TEOS ratio for silica gels after heating to 650°C.

Figure 8 — TEM of silica gel from a solution with H_2O/TEOS = 2 after drying at 85°C.

Figure 9 — TEM of silica gel from a solution with H_2O/TEOS = 2 after heating to 850°C.

FIG. 1

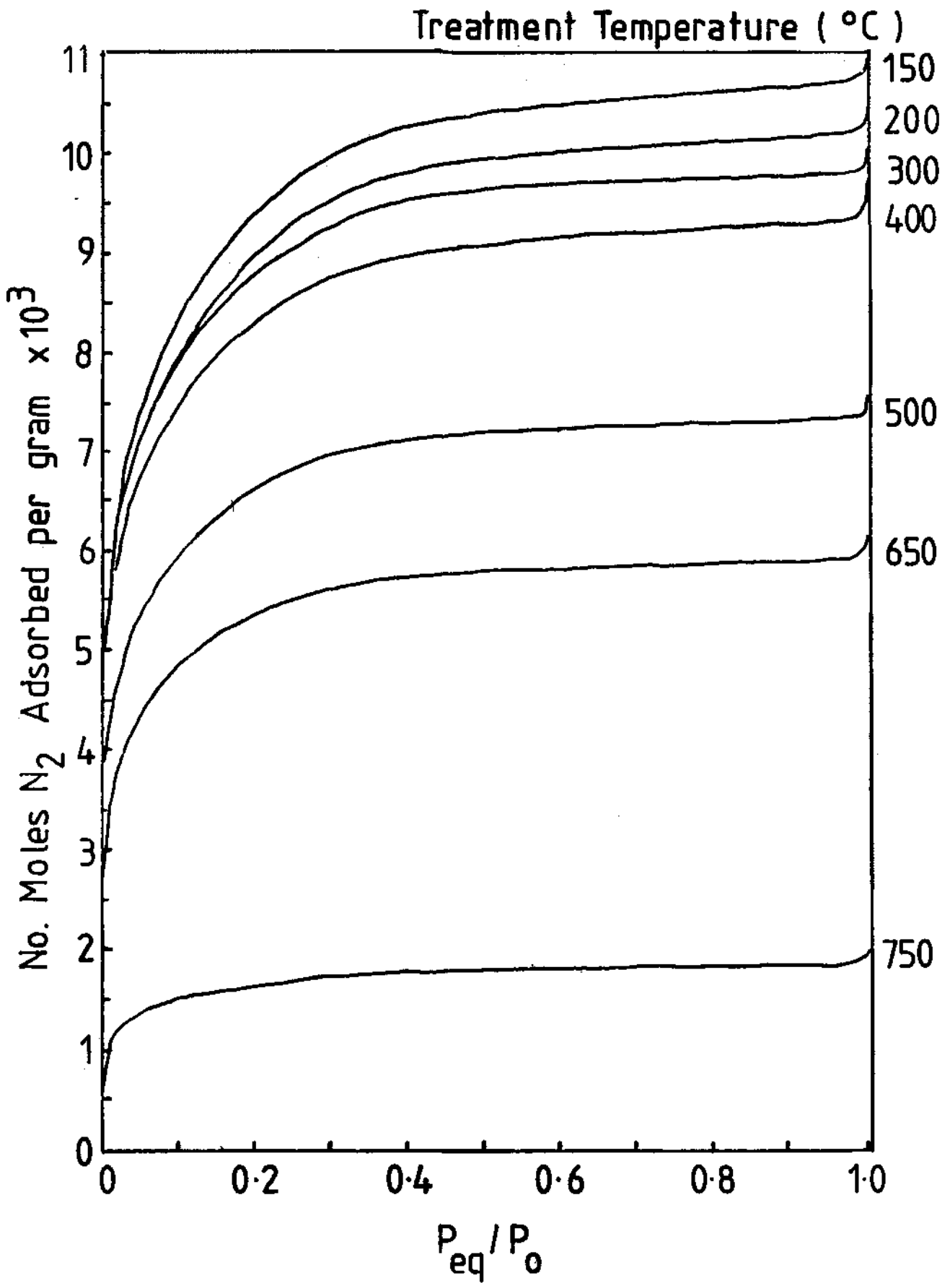
Treatment Temperature (°C)
150
200
300
400
500
650
750
No. Moles N_2 Adsorbed per gram x 10^3
0
1
2
3
4
5
6
7
8
9
10
11
0
0·2
0·4
0·6
0·8
1·0
P_{eq} / P_o

FIG. 2

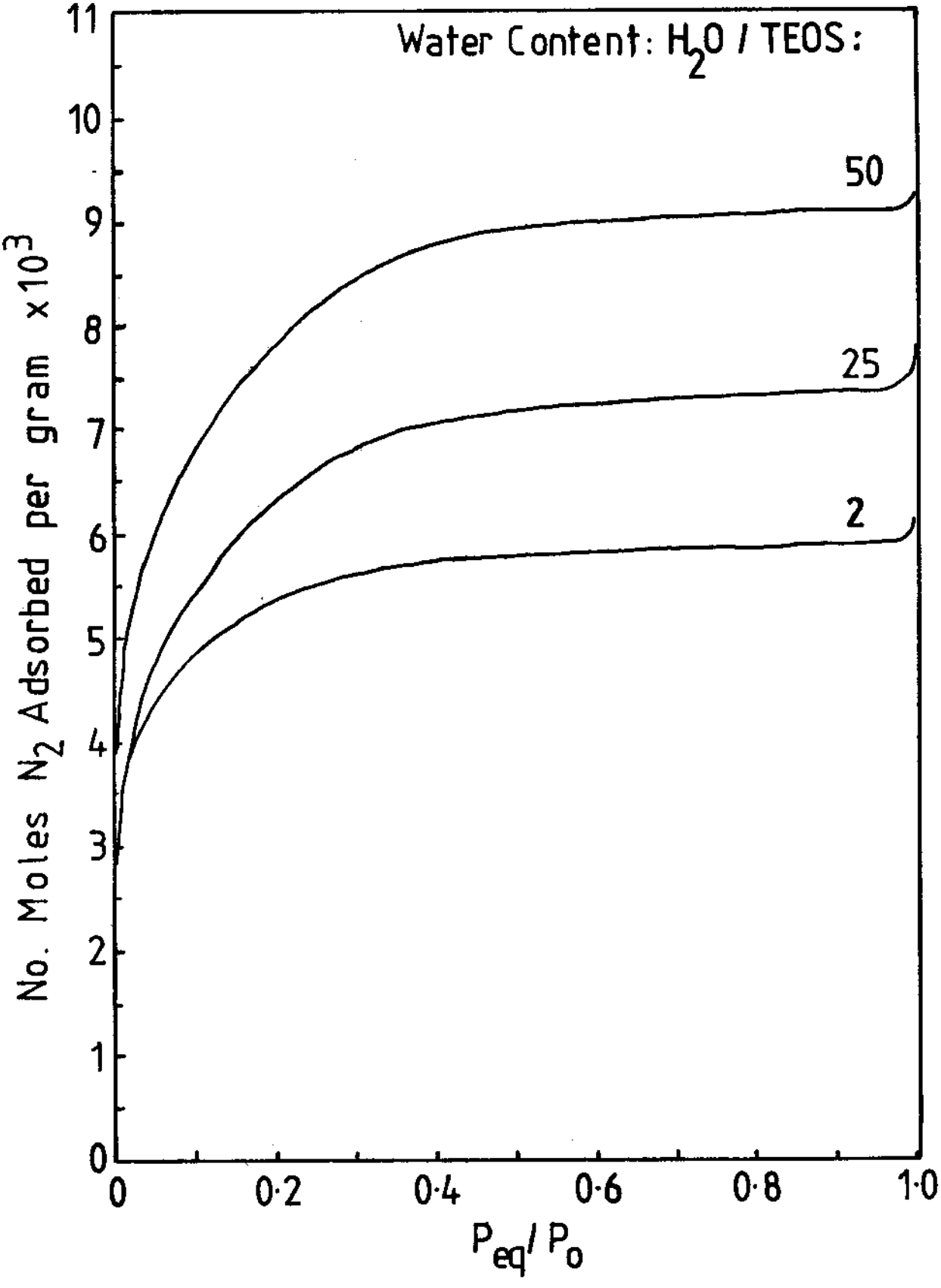
Water Content: H_2O / TEOS:
50
25
2
No. Moles N_2 Adsorbed per gram $\times 10^3$
0
1
2
3
4
5
6
7
8
9
10
11
0
0·2
0·4
0·6
0·8
1·0
P_{eq}/P_o

FIG. 3

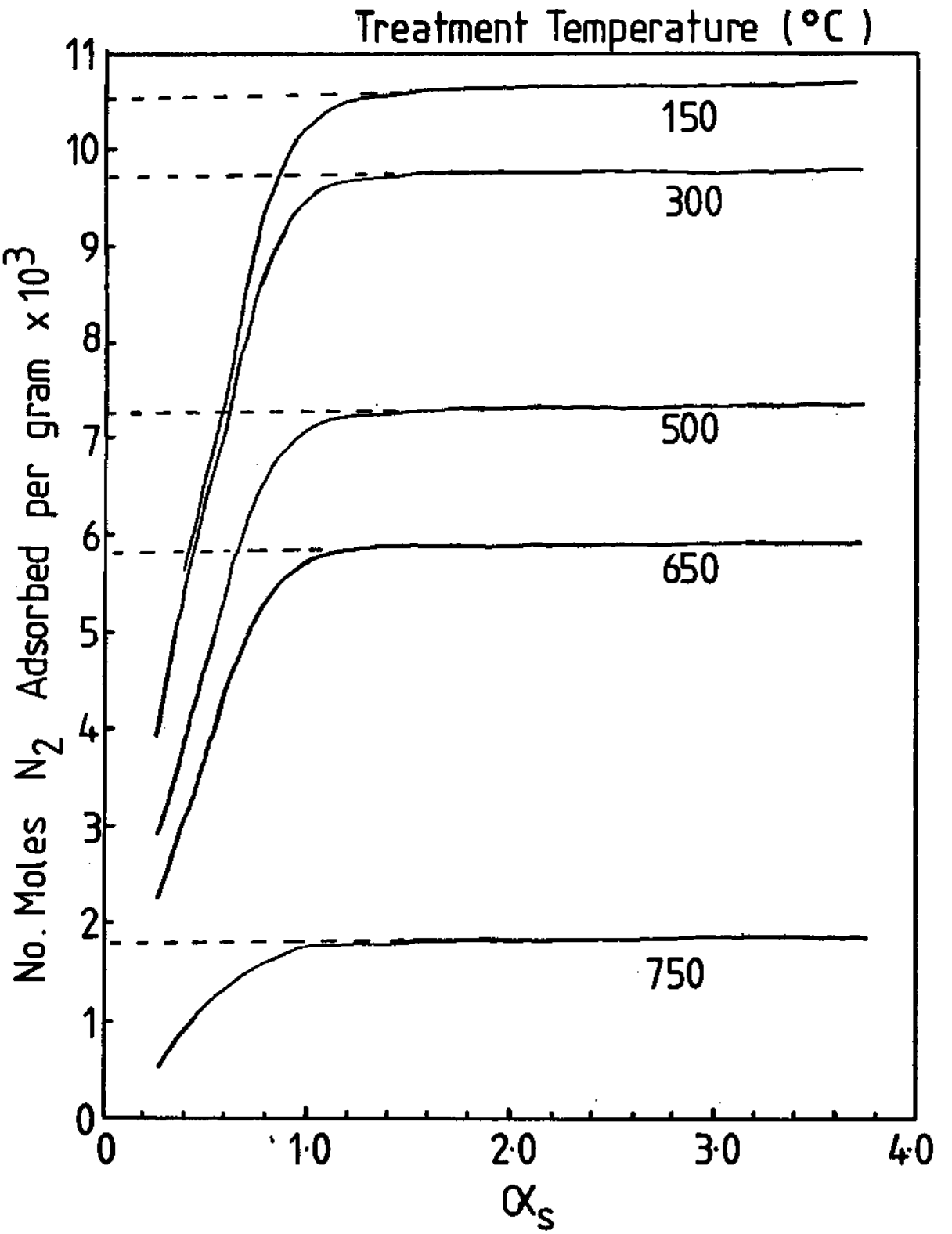
Treatment Temperature (°C)
150
300
500
650
750
No. Moles N_2 Adsorbed per gram x 10^3
α_s
0
1·0
2·0
3·0
4·0
1
2
3
4
5
6
7
8
9
10
11

FIG. 4

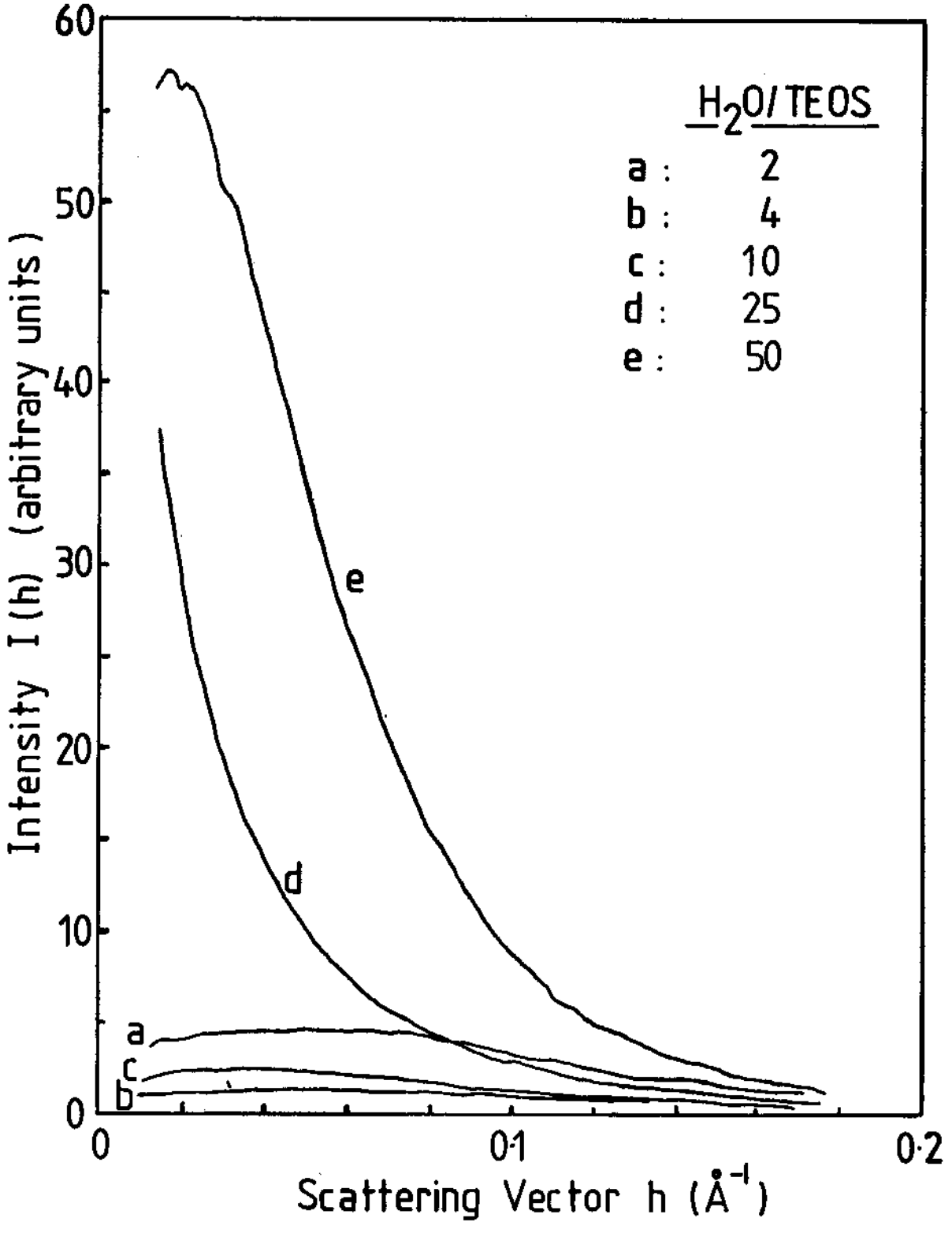
H2O/TEOS
a : 2
b : 4
c : 10
d : 25
e : 50
Intensity I(h) (arbitrary units)
Scattering Vector h (Å⁻¹)
0
10
20
30
40
50
60
0
0·1
0·2
a
b
c
d
e

FIG. 5

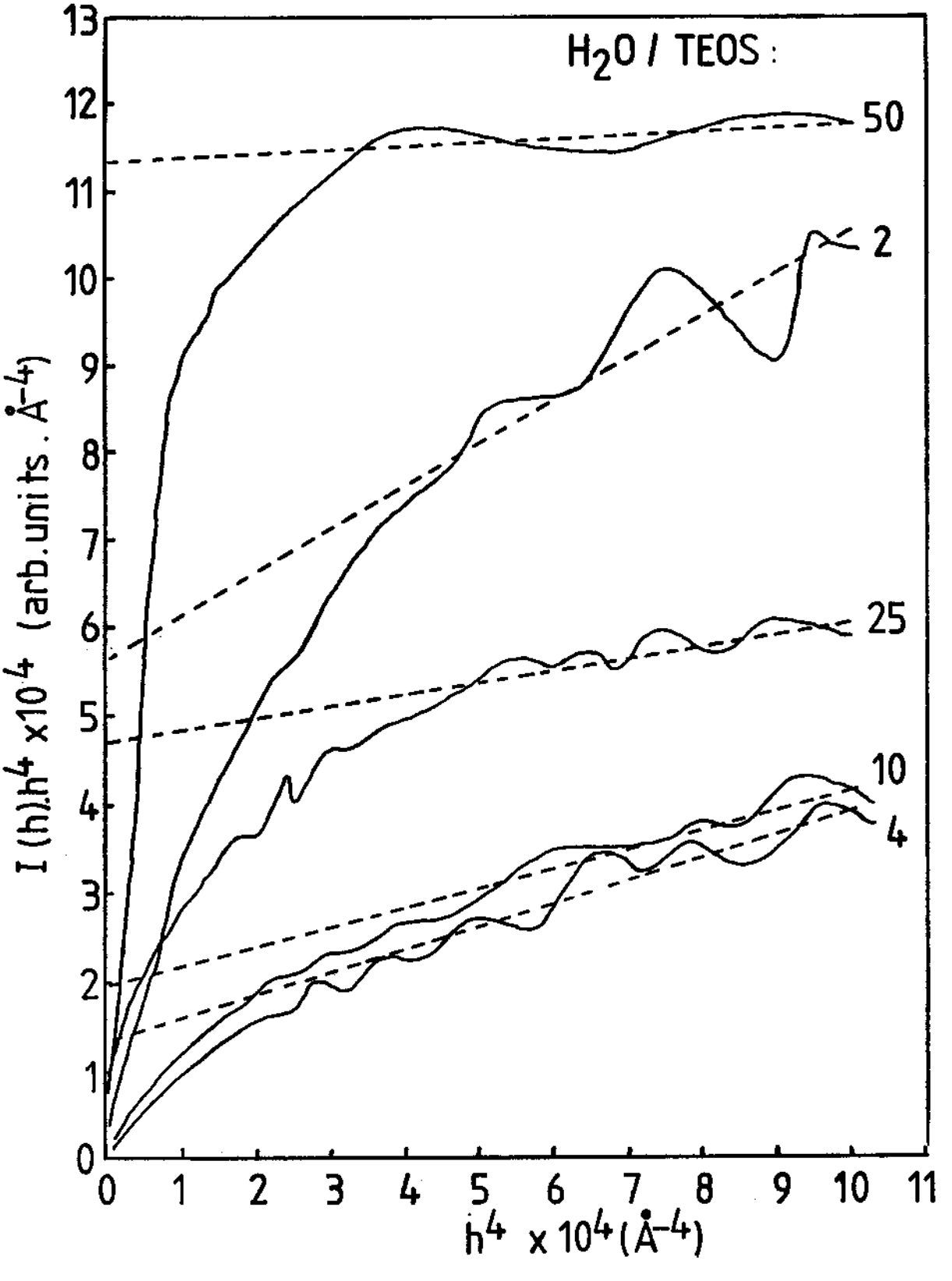
H2O / TEOS :
50
2
25
10
4
I (h).h4 x10-4 (arb.units . Å-4)
h4 x 10-4 (Å-4)
0
1
2
3
4
5
6
7
8
9
10
11
12
13

FIG. 6

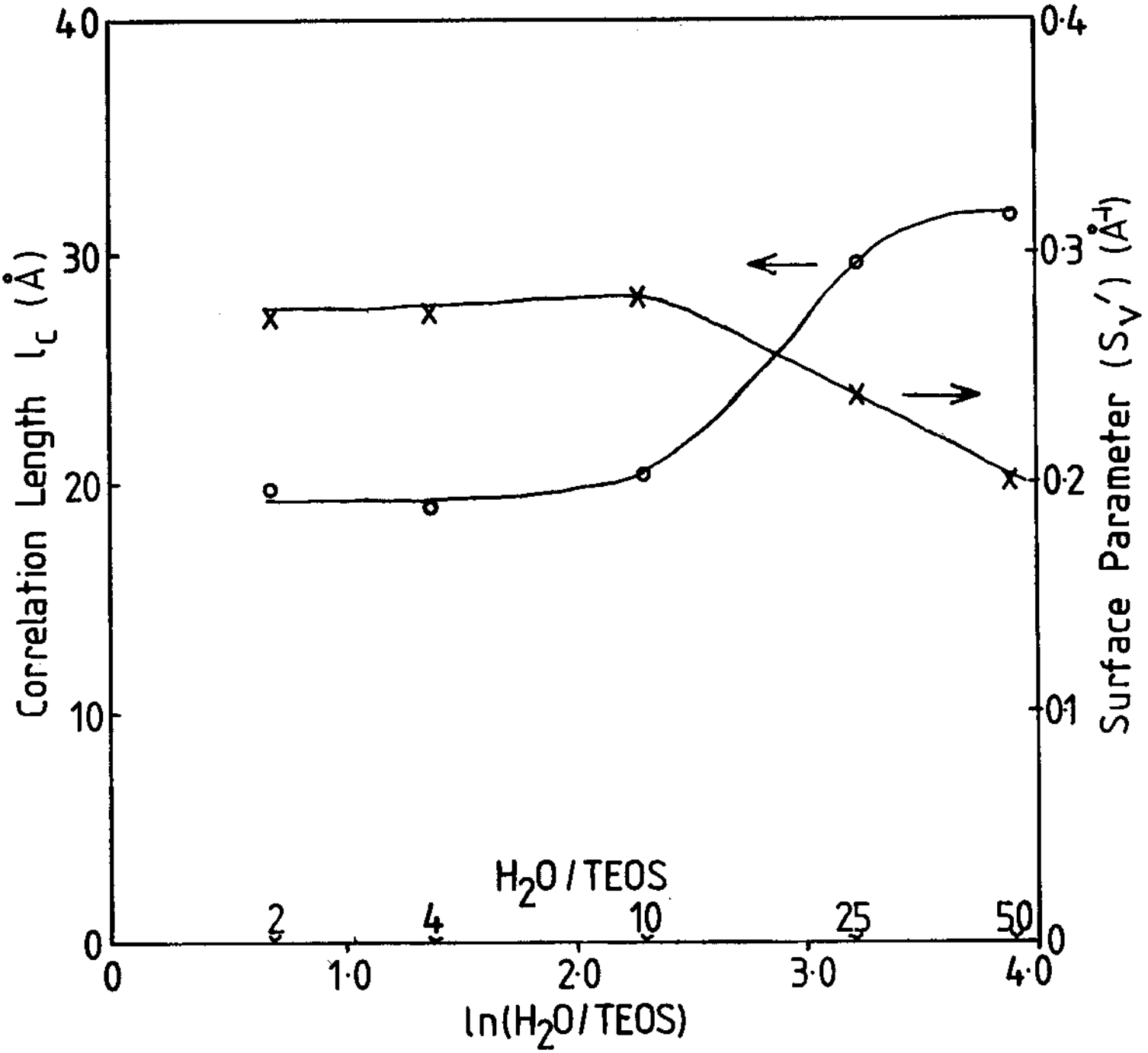
40
30
20
10
0
0·4
0·3
0·2
0·1
0
Correlation Length l_c (Å)
Surface Parameter (S_V') (Å^{-1})
H_2O / TEOS
2
4
10
25
50
0
1·0
2·0
3·0
4·0
ln(H_2O/TEOS)

FIG. 7

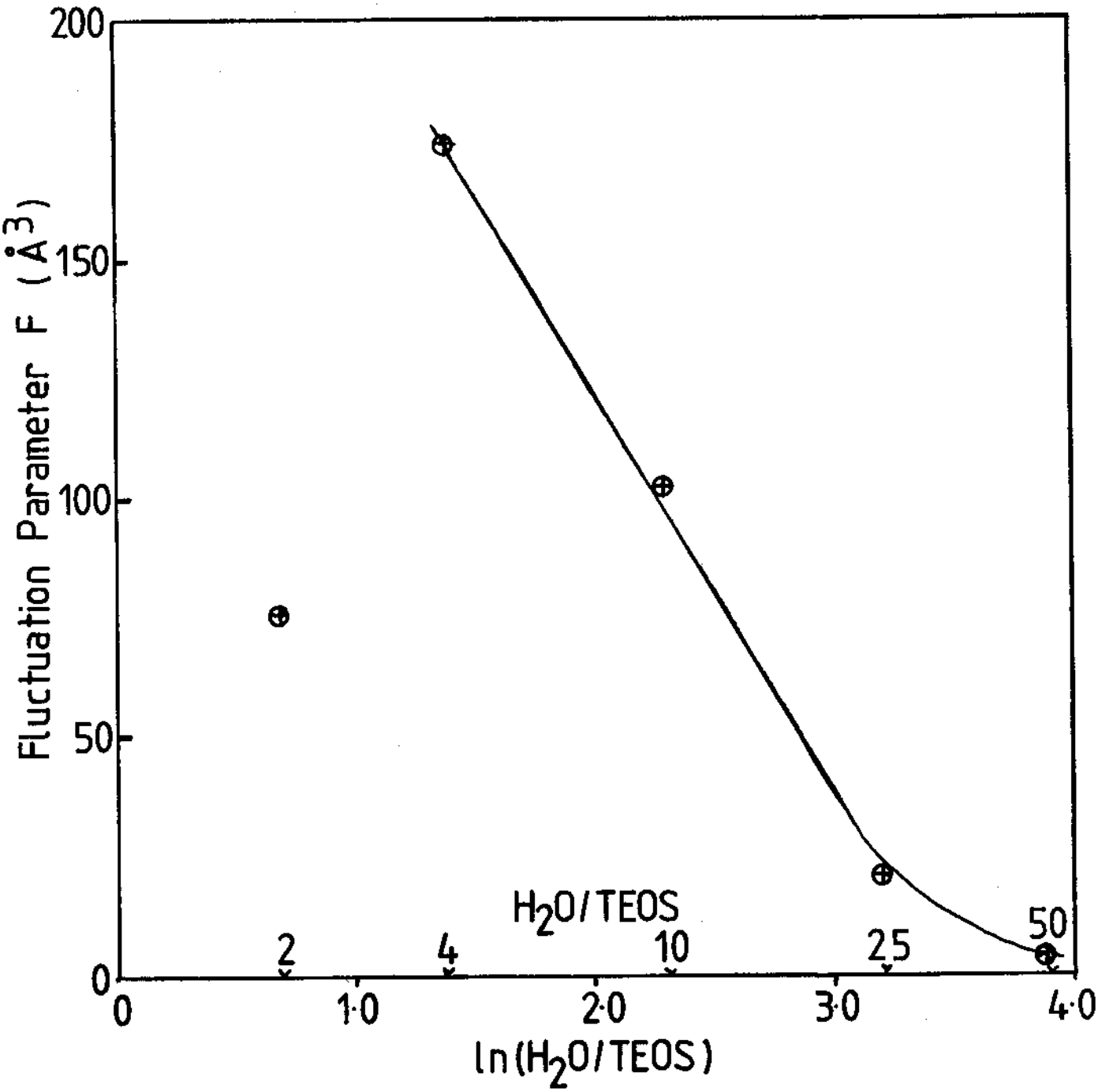
200
150
100
50
0
Fluctuation Parameter F (Å3)
H2O/TEOS
2
4
10
25
50
0
1·0
2·0
3·0
4·0
ln(H2O/TEOS)

FIG. 8

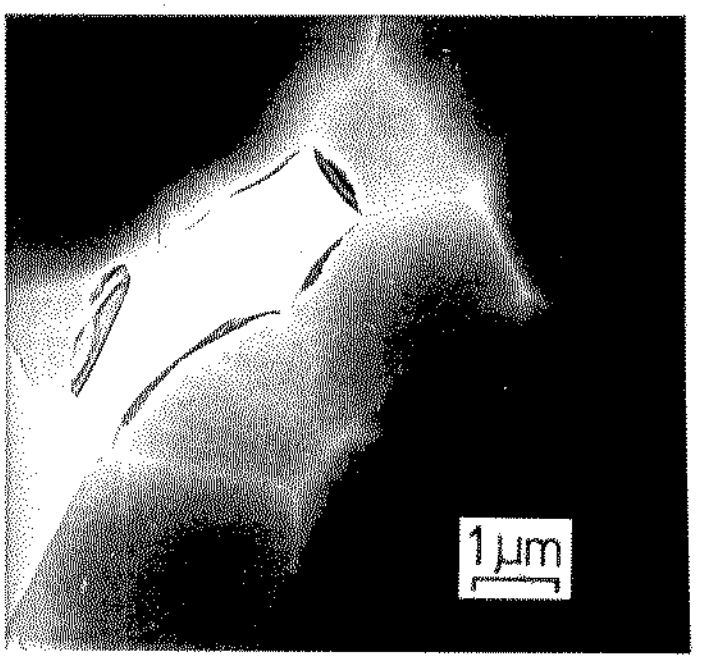

FIG. 9

Table 1

Composition of Solutions used to Prepare Silica Gels

	Composition (ml)				
Designation	$SiO_2.2H_2O$	PS1	PS2	PS3	PS4
TEOS	11.94	10.57	8.78	6.18	4.13
EtOH	11.07	10.57	8.78	6.18	4.13
HCl (conc)	1.67	0.48	0.42	0.28	0.19
H_2O	0.33	3.38	7.02	12.36	16.52
Nominal H_2O/TEOS	2	4	10	25	50

Table 2

Molarities of the Components in the Silica Forming Solutions

	$SiO_2 2H_2O$	PS1	PS2	PS3	PS4
Component					
TEOS	2.13 M	1.89 M	1.57 M	1.10 M	0.74 M
EtOH	7.58 M	7.24 M	6.00 M	4.24 M	2.84 M
HCl	0.66 M	0.19 M	0.16 M	0.11 M	0.07 M
H_2O*	3.70 M	8.36 M	16.32 M	27.96 M	37.08 M
H_2O/TEOS	1.74	4.42	10.38	25.33	50.05
HCl/TEOS	0.31	0.1	0.1	0.1	0.1
Conc SiO_2% w/v	12.8	11.3	9.4	6.6	4.4

* Water concentrations are calculated on the basis:
moles $H_2O = v_{HCl} \times \rho_{HCl} (1 - wt\%/100)/18.01 + v_{H_2O}/18.01$,
where for conc HCl, $\rho_{HCl} = 1.16$ g/ml and wt% = 31.

Table 3

Micropore volume, external surface and macropore volume of the silica gels

Sample	H_2O/TEOS	Temperature °C	Micropore volume (ml/g)	Surface not in micropores m^2/g)	Macropore volume (ml/g)
$SiO_2.2H_2O$	2	150	0.364	2.98	0.0097
		200	0.347	2.70	0.0129
		300	0.336	1.31	0.0056
		400	0.317	2.63	0.0278
		500	0.251	1.34	0.0064
		650	0.201	1.85	0.0080
		750	0.063	0.87	0.0064
$SiO_2.2H_2O$	2	650	0.201	1.85	0.0080
PS3	25	650	0.252	1.51	0.0132
PS4	50	650	0.313	1.13	0.0085

Table 4

Parameters obtained from the analysis of the SAXS curves

Temperature °C H_2O/TEOS	400	500	650	750	900	
2	15.7 22.0 0.223 87		13.0 19.7 0.272 76	16.2 20.8 0.273 119		R_g ℓ_c S_v' F
4		14.4 19.8 0.259 172	12.1 19.2 0.276 174	15.9 21.2 0.265 69		R_g ℓ_c S_v' F
10		18.8 21.3 0.246 136	14.4 20.5 0.282 102	13.2 19.6 0.291 92		R_g ℓ_c S_v' F
25			36.9 29.6 0.238 21		21.5 27.8 0.225 ~0	R_g ℓ_c S_v' F
50			25.2 31.5 0.202 2		26.3 33.4 0.194 ~0	R_g ℓ_c S_v' F

Radius of gyration (R_g) determined from Guinier plots.

R_g and correlation length (ℓ_c) are in Å.

Surface parameter S_v' is in $Å^{-1}$, and fluctuation parameter F is in $Å^3$.

Table 5

Densities of Silica Gels

Sample	H_2O/TEOS	Density (g/ml) after heat treatment (°C)					
		150	300	500	650	750	900
$SiO_2.2H_2O$	2	1.14	1.24	1.37	1.39	1.80	–
PS1	4		1.43	1.51	1.55	1.69	–
PS2	10		1.40	1.53	1.65	1.73	–
PS3	25		1.13	1.24	1.38	1.64	1.69
PS4	50		1.22	1.23	1.30	1.38	1.59

Table 6

Calculated Matrix Densities and Unaccounted Volumes

Temperature °C (H_2O/TEOS)	Pore Volume ml/g micro	macro	Bulk Density g/ml	Matrix Density g/ml	Unaccounted Volume ml/g
$SiO_2.2H_2O$ (2)					
150	0.364	0.0097	1.14	1.99	0.0489
300	0.336	0.0056	1.24	2.15	0.0103
500	0.251	0.0064	1.37	2.11	0.0180
650	0.201	0.0080	1.39	1.96	0.0559
750	0.063	0.0064	1.80	2.06	0.0316
PS3 650°C (25)	0.252	0.0132	1.38	2.18	0.0049
PS4 650°C (50)	0.313	0.0085	1.30	2.23	0

Table 7

Surface Areas Calculated from SAXS Measurements

H_2O/TEOS Temperature °C	S_V' ($\AA^{-1}$)	Pore volume (ml/g)	ρ (g/ml)	ϕ_1	S(m^2/g) from eqn. [3]
2 (650°C)	0.272	0.201	1.39	0.279	394
25 (650°C)	0.288	0.252	1.38	0.348	391
50 (650°C)	0.202	0.313	1.30	0.407	375
2 (750°C)	0.273	0.063	1.80	0.113	152

Table 8

Particle size and pore size for silica gels after heating to 650°C

Sample H_2O/TEOS	Particle diameter 2R (from eqn. [6])	Pore diameter	Correlation length ℓ_c (from eqn. [1])
25	48 Å	25.6 Å	29.6 Å
50	52 Å	27.6 Å	31.5 Å

References

1. S. Sakka and K. Kamiya, Proc. Int. Symp. Factors in Densification and Sintering of Oxide and Non-oxide Ceramics, Hakone, Japan (1978) 101.

2. K. Kamiya, S. Sakka and M. Mizutani, Yogyo-Kyokai-Shi, 86 (1978) 553.

3. N. Nogami and Y. Moriya, J. Non-Crystalline Solids, 37 (1980) 191.

4. M. Yamane, S. Aso, S. Okano and T. Sakaino, J. Mat. Sci., 14 (1979) 607.

5. M. Yamane, S. Aso, and T. Sakaino, J. Mat. Sci., 13 (1978) 865.

6. T. Kawaguchi, H. Hishikura, J. Irua and Y. Kokubu, J. Non-crystalline Solids, 63 (1984) 61.

7. D.M. Krol and J.G. van Lierop, J. Non-crystalline Solids, 63 (1984) 131.

8. B.E. Yoldas, Bull. Am. Ceram. Soc., 54 (1975) 286.

9. C.J. Brinker, K.D. Keefer, R.A. Assink, B.D. Kay and C.S. Ashley, J. Non-crystalline Solids, 63 (1984) 45.

10. C.J. Brinker and S.P. Mukherjee, J. Mat. Sci., 16 (1981) 1980.

11. S. Brunauer, L.S. Deming, W.S. Deming and E. Teller, J. Am. Chem. Soc., 62 (1940) 1723.

12. S.J. Gregg and K.S.W. Sing, "Adsorption, Surface Area and Porosity", Academic Press, (1967).

13. S. Brunauer, P.H. Emmett and E. Teller, J. Am. Chem. Soc., 60 (1938) 309.

14. I. Langmuir, J. Am. Chem. Soc., 38 (1916) 2221.

15. B.C. Lippens and J.H. de Boer, J. Catalysis 4 (1965) 319.

16. K.S.W. Sing, Chem. Ind. (London), (1968) 1520.

17. C.J. Brinker, K.D. Keefer, D.W. Shaefer and C.S. Ashley, J. Non-crystalline Solids, 48 (1982) 47.

18. M. Yamane, S. Inoue and A. Yasumori, J. Non-crystalline Solids, 63 (1984) 13.

19. P. Yu, H. Lui and Y. Wang, J. Non-crystalline Solids, 52 (1982) 511.

20. A. Guinier, "Theorie et Technique de la Radiocrystallographie", Dunod, Paris (1964).

21. G. Porod, Kolloid Z., 124 (1951) 83.

22. N. Tohge, G.S. Moore and J.D. Mackenzie, J. Non-crystalline Solids, 63 (1984) 95.

23. C.J.R. Gonzalez-Oliver, P.F. James and H. Rawson, J. Non-crystalline Solids, 48 (1982) 129.

24. J.D. Carruthers, P.A. Cutting, R.E. Day, M.R. Harris, S.A. Mitchell and K.S.W. Sing, Chem. Ind. (London), (1968) 1772.

25. E.D. Zanotto, Ph.D. Thesis, University of Sheffield, (1982).

26. O. Glatter and O. Kratky, "Small Angle X-ray Scattering", Academic Press, London (1983).

27. W. Ruland, J. App. Cryst., 4 (1971) 70.

28. R. Aelion, A. Loebel and F. Eirich,. J. Am. Chem. Soc., 72 (1950) 5705.

29. R.K. Iler, "The Chemistry of Silica", J. Wiley, New York (1979).

30. R.G. Avery and J.D.F. Ramsay, J. Colloid Interf. Sci., 42 (1973) 597.